Journal of Colloid and Interface Science 588 (2021) 401–417

Contents lists available at ScienceDirect

Journal of Colloid and Interface Science

journal homepage: www.elsevier.com/locate/jcis

Regular Article

Measuring particle size distribution and mass concentration of nanoplastics and microplastics: addressing some analytical challenges in the sub-micron size range

F. Caputo [a,*], R. Vogel [b,c], J. Savage [d], G. Vella [d], A. Law [e], G. Della Camera [f], G. Hannon [d], B. Peacock [e], D. Mehn [g], J. Ponti [g], O. Geiss [g], D. Aubert [e], A. Prina-Mello [d,h], L. Calzolai [g]

[a] Department of Biotechnology and Nanomedicine, SINTEF Industry, Trondheim, Norway
[b] School of Mathematics and Physics, The University of Queensland, St Lucia, QLD 4072, Australia
[c] IZON Science Ltd., Burnside, Christchurch 8053, New Zealand
[d] LBCAM, Department of Clinical Medicine, Trinity Translational Medicine Institute, Trinity College Dublin, Dublin, Ireland
[e] NanoFCM Co., Ltd, Medicity, Building D6, Thane Road, Nottingham NG90 6BH, UK
[f] Institute of Biochemistry and Cell Biology, CNR, Via P. Castellino 111, 80131 Napoli, Italy
[g] European Commission, Joint Research Centre (JRC), Ispra, Italy
[h] AMBER Centre, CRANN Institute, Trinity College Dublin, Dublin, Ireland

GRAPHICAL ABSTRACT

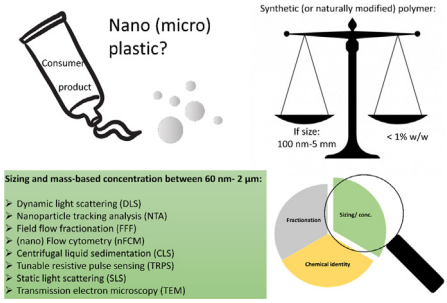

ARTICLE INFO

Article history:
Received 8 October 2020
Revised 7 December 2020
Accepted 14 December 2020

ABSTRACT

Hypothesis: The implementation of the proposal from the European Chemical Agency (ECHA) to restrict the use of nanoplastics (NP) and microplastics (MP) in consumer products will require reliable methods to perform size and mass-based concentration measurements. Analytical challenges arise at the nanometre to micrometre interface, e.g., 800 nm–10 μm, where techniques applicable at the nanometre scale reach their upper limit of applicability and approaches applicable at the micrometre scale must be pushed to their lower limits of detection.

Abbreviations: AF4, Asymmetric flow field flow fractionation; CLS, Centrifugal liquid sedimentation; CoV, Coefficient of variation; Dg, Geometric diameter or diameter of gyration; Dh, Hydrodynamic diameter; DLS, Dynamic light scattering; ECHA, European Chemicals Agency; EM, Electron microscopy; FCM, Flow cytometry; MADLS, Multi-angle dynamic light scattering; MALS, Multi angle light scattering; MP, Microplastic; nFCM, Nanoflowcytometry; NP, Nanoplastic; NTA, Nanoparticle tracking analysis; PCD, Particle concentration distribution; PE, Polyethylene; PET, Polyethylene terephthalate; PP, Polypropylene; PS, Polystyrene; PSD, Particle size distribution; SLS, Static light scattering; TEM, Transmission electron microscopy; TRPS, Tunable resistive pulse sensing.

* Corresponding author.
E-mail address: fanny.caputo@sintef.no (F. Caputo).

https://doi.org/10.1016/j.jcis.2020.12.039

Keywords:
Nanoplastic
Microplastic
Particle size distribution
Particle concentration
Regulation
ECHA microplastic restriction
Risk assessment

Experiments: Herein, we compared the performances of nine analytical techniques by measuring the particle size distribution and mass-based concentration of polystyrene mixtures containing both nano and microparticles, with the educational aim to underline applicability and limitations of each technique.
Findings: Light scattering-based measurements do not have the resolution to distinguish multiple populations in polydisperse samples. Nanoparticle tracking analysis (NTA), nano-flowcytometry (nFCM) and asymmetric flow field flow fractionation hyphenated with multiangle light scattering (AF4-MALS) cannot measure particles in the micrometre range. Static light scattering (SLS) is not able to accurately detect particles below 200 nm, and similarly to transmission electron microscopy (TEM) and flow cytometry (FCM), is not suitable for accurate mass-based concentration measurements. Alternatives for high-resolution sizing and concentration measurements in the size range between 60 nm and 5 μm are tunable resistive pulse sensing (TRPS) and centrifugal liquid sedimentation (CLS), that can bridge the gap between the nanometre and micrometre range.

1. Introduction

1.1. Microplastics and nanoplastics threat: reasoning behind the ECHA proposed restriction

The terms 'microplastic' (MP) usually refers to small, microscopic (<5 mm), solid particles made of non-biodegradable synthetic polymers. MPs are either intentionally added to consumer products (primary MP) or unintentionally generated by degradation of bulk plastic litter, as a consequence of inappropriate or ineffective disposal in the environment and in-use degradation, e.g. from textiles and tyres (secondary MP).

Once released or generated by litter degradation, they are associated with long-term persistence in the environment. MP particles have been detected in multiple environmental settings, including fresh- and sea water, atmosphere, sediments, soils, sewage sludge, biota, and food [1–7]. Their presence may cause adverse effects to wide range of organisms, including invertebrates, fish, marine reptiles, birds and cetaceans, either directly or via trophic transfer. Humans are also likely to be exposed to MP, via their diet [4,6–9]. The reported negative environmental effects of MP seem rather alarming. As recently summarized by a report of the European Chemical Agency (ECHA), MP particle ingestion have been documented in more than 220 species [10–12]. Particle translocation has been observed in multiple organisms, and trophic transfer of microplastics through food chains, including both aquatic and terrestrial food chains, have been demonstrated [10–12]. Ecotoxicity testing with MP conducted on multiple species, from, zooplankton, crustaceans, algae, mussels and fish has reported toxic effects after short-term (acute) exposures. It is important to highlight that results published by many studies should be treated with caution. They are often limited by the use of unrealistically high exposure doses, and by lack of standardized analytical methods for measuring and reporting the particle physico-chemical properties in relevant environmental media, including size, shape, agglomeration state and concentrations [2,6,13–15]. Moreover, when experiments are performed in the field (e.g. in marine environments) the harmonization of biomonitoring control as well as the comparability between different sampling sites is envisaged to increase the ecological relevance and robustness of the assessment [16]. Nevertheless, some issues have been identified. First, there is strong evidence, showing that MP particles can act as concentrator of different pollutants adsorbed on the particle surface, including polycyclic aromatic hydrocarbons (PAH), polychlorinated biphenyls (PCB), organochlorine pesticides, polybrominated diphenyl ethers (PBDEs), and heavy metals [7,17–22]. They can also be a source of plasticizers [23], that are released in the organisms after particle ingestion and uptake [10–12]. Second, shape and surface area influence the toxicity profile, with smaller particles and non-spherical shapes being a potential major source of risk [10,12,13,16].

For this reason, attention is now rapidly shifting towards the even smaller plastic particles in the sub-micron range, the nanoplastics (NPs). There is still debate about the definition of the term NP, with some authors suggesting to define NP as polymer particles that present colloid behaviour within the size range of 1–1000 nm (definition used in this paper NP: 1 nm–1 μm, MP = 1 μm-5 mm) [24] and others that define particles between 100 nm and 1 μm as sub-micron plastics or MP, and particles below 100 nm as NPs [25]. Independently from the nomenclature used to define NP particles according to their size, their accumulation in the environment and the risk associated to accidental exposure to humans and wildlife is raising concern among the general public and awareness of the regulatory authorities [10–12]. The presence of NP in sea water was only recently detected [24,26]. NP particles may have a greater impact on the environment and on human health than MP; nonetheless this is still to be ascertained. Due to their smaller dimensions and specific colloidal properties NPs could pose increased hazard to the environment and biota. Moreover, the NPs high surface area would increase the likelihood of adsorption of contaminants on their surface, and the release of contaminants contained in the particles [24]. In fact, pollutant adsorption and release from plastic particles will depend, among other parameters, on the total surface area, and thus on the size of the particles. However, information on the role that these materials could play in the bioaccumulation and transport of environmental pollutants or plastic additives is lacking, due to the absence of robust methods for NP detection, identification and for the quantification of the contaminates absorbed on their surface. This lack highlights the need for the accurate measurement of both mass and particle size distribution of plastic particles in relevant media. This will pave the way to properly assess eventual plastic toxicity and to be able to use the proper metric when comparing the relative effect of different plastic particles on organisms in the environment.

Even if a quantitative risk assessment of NP and MP exposure is not practicable due to lack of methods and reliable data, the potential hazard, coupled with the foreseen increased exposure to MP and NP is considered a concrete threat by national and international authorities. In fact, the quantity of intentionally added NP and MP, released into the environment from consumer, agricultural and industrial products under reasonably foreseeable conditions of use, is estimated to be close to 36,000 tonnes per year (with a range of around 10,000 – 60,000 tonnes per year) [27]. The environmental release of intentionally added MP and NP is estimated to be less than 10% of the mass of secondary MP coming from degradation of bulk plastic litter [10,28]. While measures to limit inappropriate or ineffective disposal of plastic litter in the

environment must be taken world-wide, an "easier" starting point from the regulatory perspective is to restrict the use of intentionally added NP and MP in consumer products. In this context, the European Chemicals Agency (ECHA) has recently proposed to restrict the use of NP and MP in products where their use inevitably results in particle release to the environment. In the current proposal [11] '(nano)microplastic' means particles containing solid polymer, to which additives or other substances may have been added, and where ≥1% w/w of particles have (i) all dimensions 0. 1 μm ≤ x ≤ 5 mm, or (ii), for fibres, a length of 0.3 μm ≤ x ≤ 15 mm and length to diameter ratio of >3." It should be noticed that, even if the restriction applies to synthetic, not biodegradable polymers, bioplastics may also be a source of microplastics [29]. Currently, ECHA's committee for risk assessment (RAC) suggested that the restriction should not apply for polymers that are (bio)degradable, according to the strict criteria based on already existing biodegradability test standards described in detail in the appendix of the restriction proposal [30]. While the new restriction, if approved in its current form, will entry into force in the near future in the European Union, some states (such as France, Sweden, UK, Canada, New Zealand and the USA) are already restricting the use of NP and MP in some consumer products, (e.g. cosmetics), via national regulations.

1.2. Methodological gaps for the identification and characterization of MPs and NPs

As shown in Fig. 1A, development of analytical tools for the detection and characterization of NP and MP particles both in consumer products and in complex environmental media needs to focus on three main pillars. *(1) sample preparation by fractionation/isolation:* NP and MP are either extracted and/or separated from the matrices (environmental media or consumer products) and eventually concentrated to detectable levels; (2) *advanced physical characterization (PC)*, including sample sizing, concentration and morphology determination; (3) *chemical identification* of all the components, including the synthetic polymers backbone but also plasticizers and other impurities contained inside the particles or adsorbed on their surface. The most promising approaches have been recently reviewed and are summarized in Fig. 1A [13,14,31]. Having robust analytical tools for all of the three characterization pillars is critically important to obtain a robust risk assessment and is required for th development and validation of specific protocols. No standardized methods are available so far.

In the case of secondary NP and MP derived from environmental degradation, challenges arise in all the three measurement pillars. First, the isolation and identification of NP and MP, extracted from environmental and biological matrices (that are mostly composed of hydrocarbon chains as the synthetic polymers) may be complicated. Furthermore, their characterization is challenging due to their very heterogeneous and unknown physical–chemical properties, caused by the transformations they undergo in the environment.

The analysis of NP and MP, that are intentionally added in consumer products is expected to be challenging, but less daunting. In fact: (1) their chemical and physical identity is generally known, and primary particles may also be available as raw material, (2) primary particles are less heterogeneous in their physical–chemical properties (compared to secondary NP and MP) and (3) the extraction procedures from commercial product matrices are expected to be less complex than from environmental ones. However, even for the less "challenging" analyses, required for control and labelling purposes of consumer products, the question arises if there are methods available to respond to the new ECHA regulatory requirements. As shown in Fig. 1B, in this context three main points need to be addressed: (1) Chemical identity - are relevant polymers present? (relevant polymer: synthetic or modified polymer that is not biodegradable); (ii) Sizing - are polymer-containing particles of the relevant size present? (relevant size proposed: 100 nm-5 mm); (3) Is the concentration limit of the relevant polymers in the relevant particles exceeded? [10–12].

1.3. Sizing and concentration measurements, what is the challenge?

From a technical perspective, the sizing analysis and quantification of the mass-based concentration of particles in the complete 100 nm to 5 mm size range requires the combination of multiple complementary approaches. In fact, no single technique is able to cover the full required size range. Particles larger than 10 μm can be analyzed with established techniques such as FT-IR microscopy, Raman (1 μm for μ-Raman) and laser diffraction, or visualized by optical microscopy (OM), which are already well known and developed techniques [12,32]. For particles smaller than 800 nm, established approaches developed in the field of nano-enabled medicinal products and of nanotoxicology can be considered, such as dynamic light scattering (DLS), nanoparticle tracking analysis (NTA), multidetector-field flow fractionation (MD-FFF), tunable resistive pulse sensing (TRPS), centrifugal approaches, electron microscopy and nano flowcytometry (nFCM) [33,34].

In the nanometric range for the measurement of particle size distribution, the most widely used technique is DLS [33,34]. Despite its known low resolution, DLS has been extensively used for the measurement of NP and of particles at nanometre to micrometre interface (800 nm-5 μm), both coming from commercial products and from environmental sources [2,14,33,35,36]. Nanoparticle tracking analysis (NTA) is another light scattering technique, based on the analysis of Brownian motion of single particles. It has been recently used in two studies to demonstrate the formation of NP particles (average size of 220 nm) during the degradation of a PS disposable coffee cup lid, monitoring the increase of particle concentration over time [37,38]. Static light scattering (SLS) is widely used for nano and micrometric particles in the 100 nm-3000 μm range. All light scattering techniques mentioned above may suffer from limited resolution, due to being ensemble rather than particle by particle measurement techniques.

Adding a fractionation step, prior to performing sizing analysis of heterogeneous samples helps to significantly increase the resolution power of the measurements by light scattering in batch mode. Asymmetric flow field flow fractionation (AF4) coupled to light scattering detectors, e.g. DLS (AF4-DLS) or static light scattering (AF4-MALS) has demonstrated its power in measuring particle size distribution for a variety of complex nanoplastic mixtures. Capability for high-resolution separation and size measurements of mixtures of NPs of different size, ranging from 10 nm to 800 nm in diameter have been reported by multiple authors [33,37]. AF4 was also widely used to isolate and collect nanoplastic from complex environmental samples and biological matrices prior to off-line analysis [28,29].

TRPS is a single particle technique that has been shown to measure the particle size distribution (PSD) and concentration of synthetic and polymeric nanoparticles. Interestingly, a tunable microfluidic RPS device with a reusable lid and base that allows the dimensions of the pore to be optimized in real time to the dimensions of the analyte, has been recently used to measure size and concentration of microplastics shed from teabags with sizes as large as 21.9 μm [38]. As an alternative approach, flow cytometry (FCM) has been used to detect extracellular vesicles and populations of plastic particles in seawater [39,40]. Less explored, but very suitable alternative approaches to consider are centrifugal liquid sedimentation (CLS) and nano flow cytometry (nFCM). Finally, to get sizing information, but also to directly visualize particle

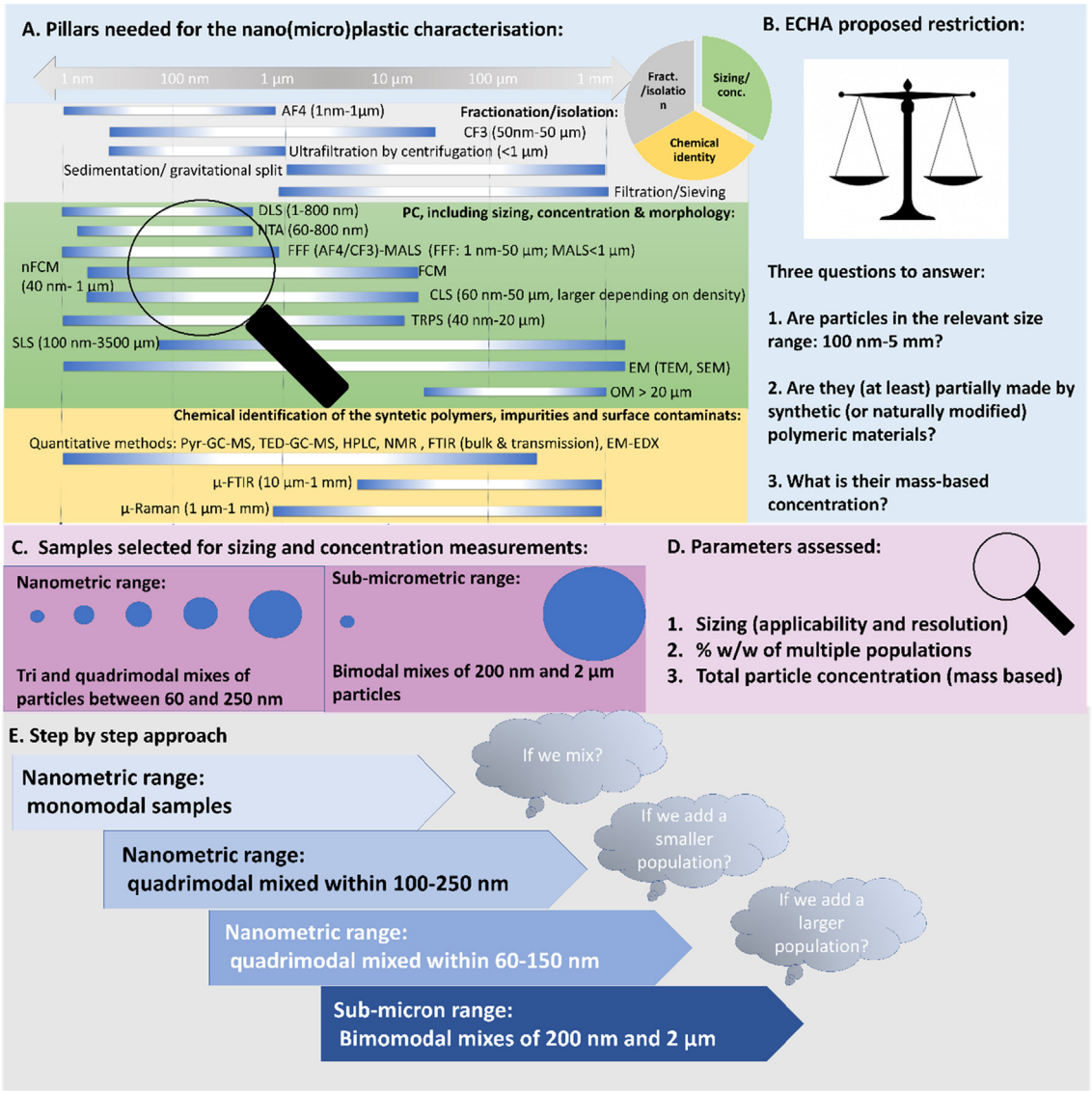

Fig. 1. Need for a robust MP and NP characterization and focus of this work. A) Overview of the techniques currently under evaluation for (i) particle fractionation/ isolation; (ii) physical characterization (PC), including sizing, particle concentration and morphology and (iii) chemical characterization. As underlined by the magnifying glass this work focuses on the sizing and concentration measurement of nanoparticles and of small micrometric particles. B) Criteria proposed in the ECHA restriction of NP and MP from consumer products, C) Summary of the nanometric and sub-micrometric multimodal mixes of NIST traceable PS particles considered in this work, D) parameter assessed for each of the steps (E). Abbreviations used: AF4 = Asymmetric field flow fractionation, CLS = Centrifugal liquid sedimentation, DLS = Dynamic light scattering, EDX = Energy-dispersive X-ray spectroscopy, EM = Electron microscopy, FCM = Flow cytometry, FTIR = Fourier transform infrared, HPLC = High pressure liquid chromatography, MADLS = Multi-angle dynamic light scattering, MALS = Multi angle light scattering, nFCM = Nanoflowcytometry, NTA = Nanoparticle tracking analysis, OM = Optical microscopy, Pyr-GC–MS =Pyrolysis gas chromatography mass spectrometry, SLS = Static light scattering, TEM = Transmission electron microscopy, TRPS = Tunable resistive pulse sensing (TRPS).

morphology, electron microscopy approaches such as scanning electron microscopy (SEM) and transmission electron microscopy (TEM) are the techniques of choice. Coupling of TEM with elemental analysis (e.g. EDX) also allows to get qualitative indications of the particle chemical nature, e.g. allowing to qualitatively distinguish polymeric particles from inorganic ones.

Each technique working in the nanometre range has its range of applicability and different capabilities to resolve complex polydisperse samples, and thus the optimal choice may be related to the properties of the analyzed samples, as reported in table S1. Importantly, the most challenging regime is the one at the nano to micro size interface (between 800 nm and 10 µm) where techniques able to measure particle size distribution and concentration at the nanoscale reach their upper limit of applicability and techniques applicable at the micro scale have to be pushed to their lower limits of detection. Detailed technical information about each of the technique selected, is reported in the supplementary section.

1.4. Chemical identification: an additional challenge

Chemical characterization should also be implemented as complementary information, for example to distinguish synthetic polymer particles from inorganic particles. Based on the need to identify synthetic polymers classical techniques such infrared spectroscopy, µ-Raman, NMR, pyrolysis GC-MS (pyr-GC-MS), and electron microscopy coupled to EDX could be used, as summarised in Fig. 1A. An extended description of the advantages and disadvantages of each of these techniques can be found in the review work by [2,13,14,31,32]. Nevertheless, it is worth noting that there are pioneering approaches combining size measurements with

chemical identification. For example, Raman spectroscopy coupled to AF4-MALS as presented by [41]. Moreover, after particle fractionation carried out by field flow fractionation and MALS online analysis, the sample fractions can be collected and analysed offline by FTIR, NMR, XPS, pyro-GC-MS, EM + EDX, and XPS. However, those are advanced hyphenated approaches, which all require validation studies to understand their applicability range and sensitivity against the total sample concentration available in a real scenario. Further considerations and analyses in this direction are ongoing and will be the subject of a follow up study.

1.5. Aim of the study

In this study, we have tested and compared nine complementary analytical techniques, including DLS and AF4-MALS but also SLS, TEM, NTA, CLS, TRPS, FCM and nFCM. The focus of this study is to investigate their applicability for the determination of nanoparticle size distribution of heterogeneous populations of polystyrene particles (PS). In addition, we want to challenge the capability of all the techniques tested to provide mass-based concentration estimates.

Currently, no standards truly representative of NP and MP used in consumer products exists that could be used for such a comparative study, being an important gap in the field. Despite being partially different in their physical–chemical nature, NIST-traceable polystyrene size standards have been chosen as materials with well-defined and reproducible properties. The benefit of using mixtures composed of multimodal traceable PS mixtures is that their PSDs and total concentrations are well known and hence performance of various platforms can be evaluated in a quantifiable way. Polystyrene is also of interest being the fourth most used synthetic polymer in consumer products after polyethylene (PE), polypropylene (PP) and polyethylene terephthalate (PET) [10,28,42].

The work was structured in 4 steps of incremental complexity (Fig. 1E). First, we have measured the size and concentration of monodispersed standards, focusing on the performances of each technique to measure not only size but also mass-based particle concentration. In the second step, we have evaluated the capability of each technique to measure highly polydisperse samples. Here we have tested quadrimodal mixtures of polystyrene standards in the 100 nm-250 nm size range (in theory well within the range of applicability of each technique tested). The polystyrene mixtures were uses as mimic for the potential polydispersity of primary and secondary NP/MP samples. Finally, we have extended the comparison of performances to smaller particles (60 nm) and to larger ones, in the sub-micron and micron range (<2 μm), by pushing detection limits of multiple techniques to the lower and to the higher end. In the latter case, our aim is to investigate what approach would be suitable for detecting MP of 1–2 μm in presence of nanoparticles. For these tests, three mixtures with variable amount of 220 nm and 2 μm were measured (see table S2).

2. Experimental

2.1. Polystyrene particles

NIST-traceable, spherical, polystyrene particles of 100 (±3) nm, 152 (±5) nm, 203 (±5) nm, 240 (±5) nm physical diameters were acquired from Thermo Fisher Scientific. Particle concentrations were provided in % (w/w) solids (1% solids in water for all above standards). The mean diameters were certified by the providers by using transmission electron microscopy (TEM). Polystyrene particles of 1.93 μm (diameter) and of 220 nm (diameter) were acquired from Polyscience. CPN220: catalogue number 07304, lot 682870: Size = 220 (±16) nm, concentration = 27 mg/ml & CPN2000 catalogue number 19814, lot 701445: Size = 1.93 (±0.06) μm, concentration = 26 mg/ml. Each of the polystyrene particle standards (CPN60, CPN100, CPN150, CPN200, CPN220, CPN240, CPN2000) was diluted and/or mixed gravimetrically using D-PBS (CaCl2 and MgCl2) + 0.03% Tween-20 to produce the subsequent mixtures in controlled w/w % ratio, as described in Table S2. The mixtures, along with the monomodal standards themselves, were subject to analysis using the different techniques listed in the table. Samples were vortexed briefly before the analysis to ensure adequate mixing and homogeneity.

2.2. Dynamic light scattering (DLS) and multi-angle dynamic light scattering (MADLS)

Prior to the measurements the samples were diluted at 50 μg/ml (total concentration) in phosphate buffer saline (PBS). Multi-angle dynamic light scattering (MADLS) was conducted on samples A and B using the Zetasizer Ultra (Malvern Panalytical, UK). Typical sample volumes were approximately 1 ml, loaded into a DTS0012 cuvette. Each sample's size distribution, particle size mode and particle concentration were measured using detectors at 3 different angles to account for front (13°), side (90°) and back (173°) scatter of light. Each sample was measured at each angle in triplicate with adaptive correlation applied to each, in order to improve overall data quality. Data was processed using the ZS Xplorer Software Suite V 1.1.0.656. The Zetasizer Ultra analysis includes total concentration, and both intensity- and volume-weighted PSDs. The volume-weighted PSDs were post-processed in order to produce respective concentration distributions. Prior to the actual measurements the MALDS instrument was calibrated for size measurements using a mix of 200 nm and 400 nm polystyrene latex microspheres (Malvern Panalytical, UK). Dynamic light scattering measurements of samples D-F were conducted using the Malvern Zetasizer ZS at two different wavelengths 633 nm and 532 nm, according to the SOP developed by the European Nanomedicine characterization Lab (EUNCL) [43,44]. For comparative purposes two angles were selected for the measurements 173° (SOP EUNCL) and at 13°, and measurements were performed by two different laboratories. PSD by intensity and by volume are reported. Volume based PSD was used to estimate w/w%, while size values reported are obtained from intensity-based PSD. The Malvern zeta sizer simulation software was used to simulate the light scattering as function of size at different angles (173° and 13°) and at different wavelength (633 nm and 532 nm) according to Mie theory. Refractive index (RI) of 1.59 and absorption (ABS) of 0.01 were used for the calculations.

2.3. Transmission electron microscopy (TEM)

TEM was used to assess the primary particles size distribution of samples containing 0.3 mg/ml of 200 nm and 2 μm polystyrene particles and a mixture 50:50 in mass of 220 nm – 2 μm; 3 μl of each suspension at the final concentration of 0.03 mg/ml (dilution in MilliQ water) were manually deposited on Formvar Carbon coated 200 mesh copper grids (Agar Scientific, Stansted, United Kingdom) pre-treated by glow discharge (30 *sec.*) and let to evaporate for 3 h at 4 °C and 3 h at 20 °C in desiccator. Samples were imaged with JEOL JEM- 2100 HR-transmission electron microscopy at 120 kV (JEOL, Italy) and analyzed by ImageJ, using NanoDefine Particle Sizers Plugin. Particle-counted: 220 nm: 1973 particles; 2 μm : 2784 particles; Mix D: 3180 particles.

2.4. Nanoparticle tracking analysis (NTA)

Sample dilutions for NTA were made up, using PBS + 0.03% Tween-20 to a working volume of 1 ml, in order to obtain an optimum particle concentration for NTA (between 10 and 50 particles per field of view). The samples (~600 μl) were then loaded into the NanoSight instrument. NTA-analyses of the polystyrene particles and of their mixtures were conducted using the NS500 NanoSight (Malvern Panalytical, UK) along with the Nanosight 3.2 software package (NTA build 3.2.16) following the European Union Nanomedicine Characterisation Laboratory (EUNCL) approved protocol [45]. A 405 nm laser was used to visualise particles, present in a given field of view. A minimum of three, 60 s recordings of the laser interacting with particles were captured using an EM-CCD camera. 100 nm and 1 μm polystyrene latex microspheres (Malvern Panalytical, UK) of known size were used as quality control for NTA measurements. For most multimodal polystyrene samples PSDs of the various modes within the mix overlapped and hence it was not possible to determine % w/w. distribution of various particle sizes in the mix. NTA was conducted for each of the polystyrene standards prior to analysis of the mixtures to give a preliminary estimation of the mode particle diameters of the monomodal standards.

2.5. Static light scattering (SLS)

A Mastersizer (Malvern) instrument equipped with a red and blue laser and a Hydro SV small volume measurement unit was used to run SLS measurements on mixtures of 200 nm and 2 μm PS particles. Stock suspensions were diluted to a concentration of 132.5 μg/ml in MilliQ water. Mixtures with a final volume of 1 ml were prepared at 0, 10, 50, 90, 99, 100% w/w of the smaller particle fraction. These mixtures were injected under stirring in 5 ml of MilliQ water placed in the measurement cell. Background and sample measurement durations were set to 10 s and 5 s for the red, 5 s and 5 s for the blue channel. Spherical particle model with 'Narrow Modes type' evaluation was selected for data analysis considering Mie theory. Optical properties for polystyrene and water were applied as pre-set material properties suggested by the software (with absorption value of 0 for PS and refractive index of 1.59 and 1.33 for PS and water, respectively). PSD results were generated considering the average of 5 measurements.

2.6. Tunable resisting pulse sensing (TRPS)

TRPS was performed with a qNano Gold (Izon Science), equipped with IZON Science Control Suite v. 3.3. The system was equipped with an air-based pressure module to apply the required pressure range. Tunable nanopores were fabricated in TPU membranes (Elastollan1160D, BASF), as detailed in [46–49]. For the measurements of mixtures within the 60 nm-250 nm size range, size and concentration calibrations were performed, using CPN100 and CPN200 standards at a concentration of 10^{10}/ml in PBS, containing surfactant (0.03 wt% Tween20). A NP150 nanopore was used for measuring samples A, B and C. In the case of the 200 nm + 2 μm mixtures, the stock solutions in PBS 1x + 0.03 w/w% Tween20 were diluted by 1:4 in MilliQ water. Two nanopores (NPs) were used for each sample (NP300 and NP2000), to cover the full-size range in the 200 nm – 2 μm range. Samples were diluted at the optimal concentration range associated to each nanopore. The results were obtained by combining the data from the two nanopore runs for each sample. The samples were analyzed without filtering any particles. Even the 200 nm + 2 μm in the 50:50 mixture was measured without need for filtration when measuring with the NP300, if care was taken to avoid and resolve pore blockages. As NP300 limits of detection/operation are typically 150–900 nm, the populations were able to be resolved only under carefully managed conditions. Standard operations with real NP and MP samples may therefore most likely require the use of two pores and prior filtration of samples. All the samples were analyzed at least in triplicates and a new calibration was performed between consecutive samples. The alternating calibration process virtually eliminates the impact of any change in pore geometry, occurring during the measurement process on particle size and concentration results and hence guarantees reliable results. All the samples were analyzed by using a multi-point pressure method [46], with pressures typically ranging between 0.3 and 2.0 kPa and typical sample volumes being 35–40 μl. The multi-point pressure method eliminates the impact of pore and particle zeta potentials (electrokinetic effects) on the measured concentration. Notably, the TRPS analysis of number-based PSD requires no data post-processing. However, in order to calculate the mass-weighted PSD, the number-based particle distribution was transformed into mass-based particle distribution, assuming a particle density of 1.05 g/L and a spherical particle shape.

2.7. Asymmetric flow field flow fractionation (AF4-MALS)

The AF4-MALS system used in this study included an Eclipse Dualtec separation system (Wyatt Technology Europe GmbH, Dernbach, Germany) and an Agilent 1260 Infinity high performance liquid chromatograph equipped with a degasser (G1322A), an isocratic pump (G1310B), an autosampler (G1329B) and a multi-wavelength detector (G1365C), all from Agilent Technologies (Agilent Technologies, Santa Clara, USA). A Dawn 8 + Heleos II multiangle laser light scattering (MALS) detector operating with a 658-nm laser (Wyatt Technology Europe) was coupled to the fractionation system. The 90° detector angle was used to monitor the signal during analysis. Regenerated cellulose (10 kDa) membranes were used in the Eclipse SC separation channel (153 mm length). The spacer height was 350 μm. The temperature of the channel was kept constant at 25 °C. The eluent was 0.05% sodium dodecyl sulphate in ultrapure water for the analysis of polystyrene samples. The flow programme and crossflow settings are reported in the Table S3. The data acquired by the online MALS detector were processed using the ASTRA® 6.1 software package (Wyatt Technology Europe). The geometric diameter (or diameter of gyration, Dg) versus time was determined by applying the Lorentz-Mie model. The total particle concentration was calculated by applying the number density model (RI = 1.59) and by integrating the peaks over time, knowing injected sample volume and AF4 volume flow rate. The differential mass-based PSDs, where the particle concentration versus size is expressed in arbitrary units, were also calculated. Low scattering intensity data is typically excluded, with the result that smaller particles in polydisperse samples may be underestimated by this calculation. The following parameters were reported:

a. Complete fractogram(s) of the eluted sample, showing the elution time on the x-axis and the detector response(s) (UV–VIS and Dg) on the y-axis (Figure S1);
b. The differential mass-based particle size distribution in arbitrary units.
c. The mode value of Dg calculated by assuming a spherical shape.
d. The w/w % distribution of the relative concentration of the different particle populations, when peaks of different populations were resolved with sufficient resolution.

AF4-MALS was not conducted on the samples containing 2 μm particles, being out of the range suitable for online MALS analysis

(applicable < 400–500 nm depending on the model used for the fitting).

2.8. Centrifugal liquid sedimentation (CLS)

Experiments were performed using a CLS Disc Centrifuge (model DC24000 UHR, CPS Instruments, Inc., USA) applying light extinction-based detection. For the separation of all the mixtures, a density gradient made of 9 steps of 1.6 ml of 0–8% sucrose solution was used at a rotation speed of 22000 rpm. Refractive indices of 1.59 and density of 1.05 g/ml were applied in the calculations for polystyrene particles. The absorption was set to 0.001. To protect the sucrose gradient against water evaporation, 0.5 ml of gradient cap fluid (dodecane, CPS Instruments, Inc.) was added on top of the last layer (8%). A CLS size calibration standard (lot. 150, CPS Instruments, Inc.), i.e., an aqueous suspension of monodisperse spherical polyvinyl chloride (PVC) particles with a diameter of 237 nm, was injected before each individual measurement, in order to determine the actual properties (density, viscosity) of the gradient. In our experiments the mass of the syringe loaded with about 100 μl suspension before injection and the mass of the syringe after injection were measured using an analytical balance. Supposing that the nanoparticles at the applied concentration have negligible effect on the effective density of the suspension, the mass measurement allows the calculation of the injected volume and thus the mass-based concentration from the mass-weighted distribution data. Post-processing of the CLS data implied an additional baseline subtraction, performed by using the Origin software.

2.9. Flow cytometry (FCM)

FCM analysis was performed using the Amnis CellStream system (Luminex, USA) and analyzed with v. 1.2.96 CellStreamAnalysis software. Samples were individually loaded at 3.66 μl per minute from a 1 ml Eppendorf. To prevent carryover, the system is washed with filtered, HPLC grade water between samples. Particle populations (200 nm and 2 μm) were graphed using FSC versus SSC plots. For measuring mixtures of populations, the filtered HPLC grade water was measured as background and 200 nm and 2 μm particles (acquired from Polyscience, US) alone were measured at various concentrations. Next, samples D-F were also diluted to various concentrations in HPLC grade water before being analyzed. The FSC versus SSC plots were used to identify the different mixture ratios.

2.10. Nano flow cytometry (nFCM)

Nano flow cytometry requires specialised equipment to apply the fundamentals of standard flow cytometry to sub-micron particles. A NanoAnalyzer N30 instrument equipped with a single 488 nm laser and single-photon counting avalanche photodiodes detectors (SPCM APDs) was used for detection of the side scatter (SSC) (band pass filter: FF01-524/24) of individual particles. HPLC grade water served as the sheath fluid via gravity feed, reducing the sample fluid diameter to ~1.4um. Blanks were measured to remove noise from the data which was generated through the nFCM Professional Suite v1.8 software. The NanoAnalyzer (nFCM) has been optimized to allow for side scatter measurements of particles down to 40 nm. Comparison to sizing standard cocktails allows for intensity measurements to be converted to size.

Particle concentration was determined by calibration with 250 nm silica nanoparticles of known particle concentration to calibrate the sample flow rate. Side scatter intensities measured for particles in mixed samples (100 nm – 240 nm) were compared to a trimodal cocktail of CPN60, CPN100, CPN150 which provided a standard curve for PS particles. These measurements were taken at a laser power of 25 mW, 0.2 ss decay, allowing for inclusion of all particles in a single 1-minute measurement.

The 200 nm/2 μm particle samples were measured at 15mW as was the four-modal size standard of CPN60, CPN100, CPN150, CPN200 which was used to generate a standard curve. Due to the upper limit of 1000 nm detection, sample D and CPN2000 were excluded from analysis as to avoid overwhelming of the detectors. As such this data is shared in the supplementary results to share experimental challenges of such technique in measuring micrometric particles.

Data processing was handled within the nFCM Professional Suite v1.8 software, with dot plots, histograms, and statistical data being provided in a single PDF. Gating within the software allows for proportional analysis of subpopulations separated by side scatter (SSC) intensities with PSD and concentrations available for each sub-population. In cases where additional contaminant particles were observed (past the frequency observed in the blanks) thresholding was applied to remove these from further processing.

2.11. Size values reported by the different techniques

For reasons of simplicity and consistency between different measurement techniques as average size values we report mode diameters as opposed to mean diameters. For near- Gaussian distributions as in case of the PS-traceable standard the discrepancy between mean and mode diameters will be typically below 3%. When comparing the size derived by different approaches, we should consider that the diameters reported are defined in different ways, depending on the physical principle used for measuring size values technique by technique. While NTA, nFCM and MADLS all measure the hydrodynamic diameter, CLS measures Stokes diameter, AF4-MALS measures the diameter of gyration, TRPS measure the geometric particle diameter (3d equivalent of the Feret diameter), and TEM the Feret diameter.

To be consistent with ECHA requirements for NP and MP analysis, whenever possible we report the mass-based distribution and the total mass concentration in ng/ml as main outcome of concentration measurements, rather than the number-based distribution (NP/ml). To directly compare the mass-based PSD obtained by different techniques, the data from different techniques have been extracted and post-processed as described below.

(a) PSD: CLS measurements result in light extinction weighted PSDs, that can be transformed into mass-based PSD and mass concentrations (aiming to fit the requirements of the suggested ECHA regulation), if the total injected mass is known. The injected sample mass was therefore measured gravimetrically, allowing to report the mass-weighted PSD in ng/nm/ml. Differently from CLS, NTA, nFCM and TRPS are number-weighted techniques that directly measure size distributions in NP/ml. To assess the amount of NP in (w/w%) the measured number-weighted PSD was converted in mass-based PSD, with the knowledge of particle density and average size, assuming a particle spherical shape (in agreement with EM observations). Additionally, histograms were converted into continuous PSDs through division by bin size, to return mass-weighted PSD that are reported in ng/nm/ml. This way NTA, nFCM and TRPS data can be directly compared with techniques such as CLS or MADLS. MADLS and DLS measurements are provided in intensity-based PSD and can be converted in volume weighted and number-weighted PSD by applying Mie/Rayleigh's theory with the knowledge of the particle refractive index. MADLS can provide information on the total particle concentration, whilst conventional single angle DLS is not capable to measure particle concentration. Hence MADLS can be converted

into mass-weighted PSD that are reported in ng/nm/ml, whilst standard DLS can only measure relative weight-based distributions in arbitrary units. SLS data is intensity-based as well but can be converted in volume-weighted PSDs. However, same as DLS, the SLS only measures relative mass-based PSD in arbitrary units. AF4-MALS PSDs come both in number-weighted and mass format in arbitrary units.

In the case of NTA, MADLS and TRPS the PSD plotted are calculated by averaging the PSD obtained by three replicate runs, while CLS is based on two runs and AF4-MALS on one single run. The results obtained by averaging three PSD against the PSD of one single run are compared in the SI (Figure S2) for sample A.

(b) Total particle mass determination: CLS, NTA, TRPS, MADLS and nFCM allow for the determination of the total particle mass (concentration μg/ml) measured, whilst DLS and FCM have not shown such capability. Total particle mass is calculated by integrating over respective mass-weighted PSD (average of the results obtained by single runs as described above). Using a proprietary method patented by Wyatt [45,47], Mie theory can be used to derive the total number of particles measured by AF4-MALS, but not the particle based total mass. When available the number-based PSD is shown in the inset of the main Figs. 2–4.

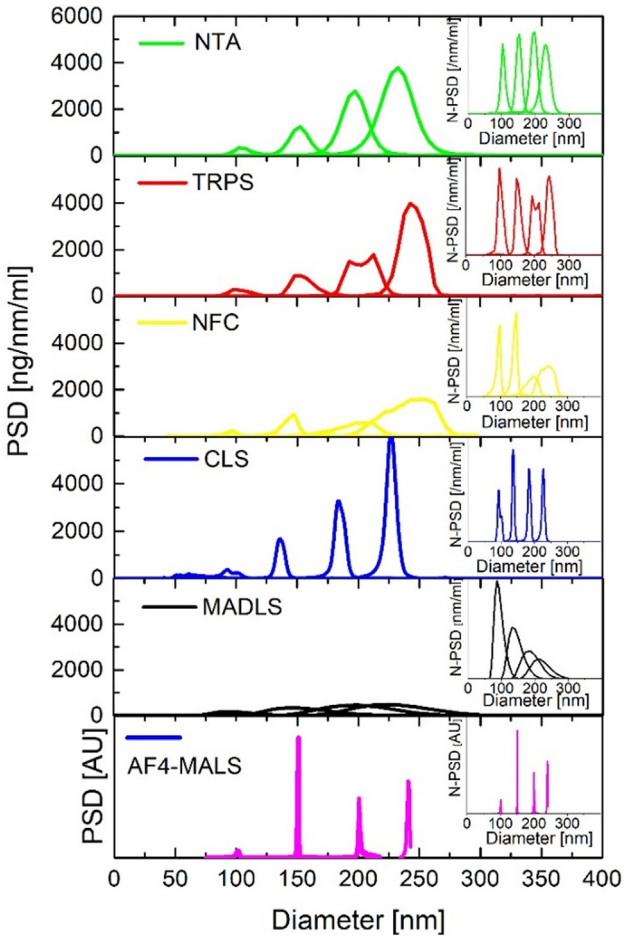

Fig. 2. NTA, TRPS, nFCM, CLS, AF4-MALS and MADLS mass-based and number-based (inset) particle size distribution measurements of monomodal CPN100, CPN150, CPN200 and CPN240. NTA, TRPS, nFCM and MADLS measurements were averaged over 3 runs and CLS over 2. For AF4-MALS the derivative PSD of a single run is reported in arbitrary units.

(c) Calculation of average size and % w/w of multimodal samples: The average mode diameter, % w/w fraction and total mass were extracted by the average PSD calculated as described in a-b). Exceptions are nFCM data, where mode diameter, % w/w fraction and total mass were extracted from 3 single runs and averaged after that. In fact, for nFCM data, loose of resolution by averaging the PSD information is more significant than for the other techniques and the analysis of three single runs is preferred not to lose information on the samples.

3. Results

3.1. Measurement of polystyrene monomodal samples in the 100–250 nm range

Mass and number-weighted size distributions of the monomodal polystyrene samples (100 nm, 152 nm, 203 nm, and 240 nm) are compared in Fig. 2, while mode diameters and total concentrations (mass- and number-based) are listed in Table 1. With regards to sizing measurements, the mode diameters of the monomodal distributions measured by NTA, TRPS, MADLS, nFCM and AF4-MALS are in close agreement (within 5%) with nominal diameters for all samples. Only CLS shows consistently smaller particle diameters (up to 11%), with a similar shift being observed in a previous comparison study [50]. In terms of the widths of the size distributions, nominal distribution standard deviations should theoretically be 7.8 nm (CV = 7.8%), 5.0 nm (3.3%), 5.3 nm (2.6%), and 3.7 nm (1.5%) for CPN100, CPN150, CPN200, and CPN240 respectively. If the expected values are compared with the measured particle size distribution widths, TRPS, NTA, CLS, nFCM and AF4-MALS are in close agreement with the nominal widths (standard deviation of the PSD), whereas MADLS PSD are far broader than the others. The total concentrations (Table 1) measured with NTA are slightly higher than the other methods for all four monomodal standards. TRPS provides accurate concentration measurements, except for 240 nm that are slightly overestimated. CLS also measure concentration precisely, except for the smaller particles tested (100 nm), where the estimated number concentration is double of the expected value. nFCM is generally slightly underestimating the total particle concentration. Finally, MADLS is significantly underestimating the concentration of larger particles. To summarize, in the case of monomodal samples < 250 nm size measurements agreed well for all tested techniques. On the other hand, particle concentration measurements are generally prone to a larger error. nFCM, TRPS and CLS are the most accurate techniques in estimating the total mass-based particle concentration (within 30%).

3.2. Measurement of polystyrene quadrimodal and trimodal samples in the nanometric range

Differently from the measurement of monomodal standards, the measurement of the PSD of a highly polydisperse sample may be very challenging. The results obtained by measuring the size and particle concentration of the multimodal samples A, B and C are reported in Fig. 3 and Fig. 4. Tabulated values of size and mass-based concentration derived are summarized in Table 1. MADLS completely fails to resolve various modes within the mixtures only showing broad distributions. This result may not be surprising for particle metrology experts, considering the known low-resolution power of batch dynamic light scattering based methods [33,34,36,51]. However, it is very important to take these limitations into consideration when analysing polydisperse samples.

NTA is another technique used by researchers to analyze NP, e.g. during the degradation of bulk plastic litter [52,53]. Herein we show that NTA cannot resolve the populations within a complex

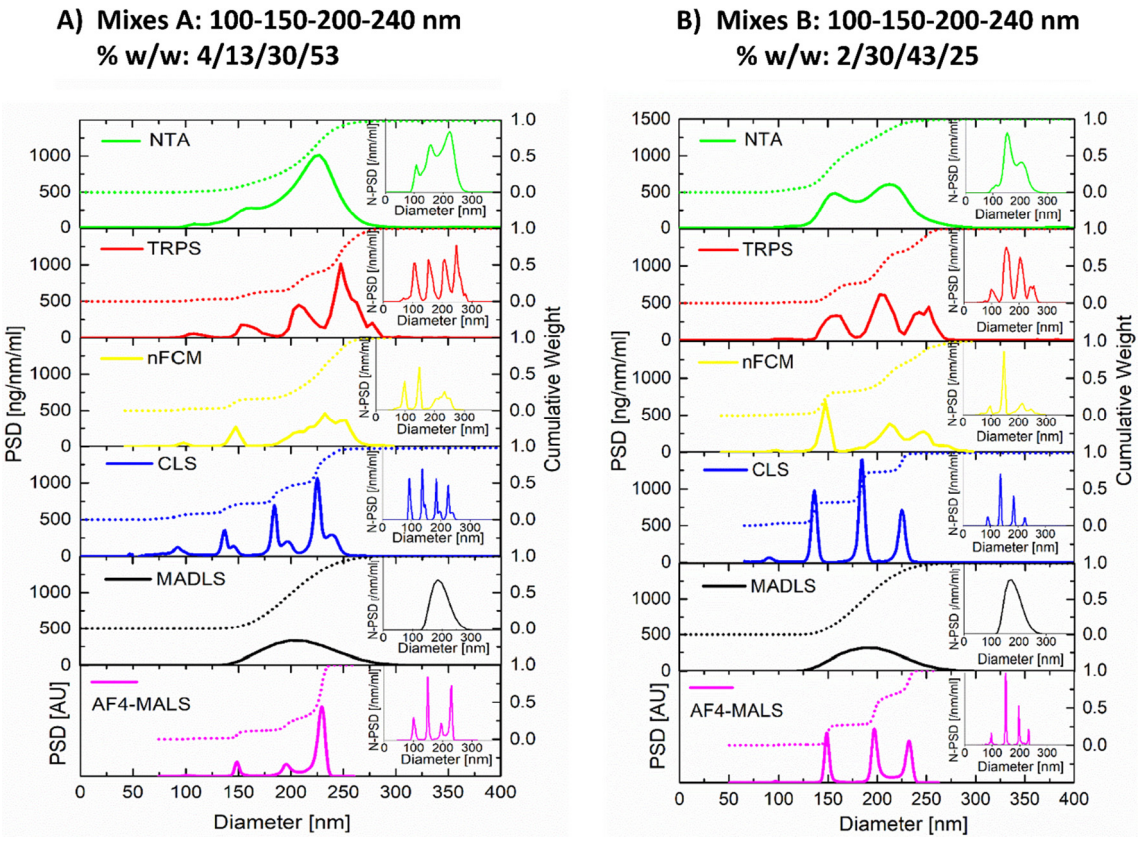

Fig. 3. NTA, TRPS, nFCM, CLS, AF4-MALS and MADLS mass-based and number-based (inset) particle size distribution measurements of samples A and B. Differential PSD (solid lines) and cumulative PSD (dotted lines) are reported. NTA, TRPS, nFCM and MADLS measurements were averaged over 3 runs and CLS over 2. For AF4-MALS PSD of a single run are reported in arbitrary units.

mixture sufficiently. To identify the different populations, the number-based PSDs obtained by NTA can be fitted with Gaussians curves in order to quantify contributions of various modes within the mix (data not shown). This is possible since the size of the different populations within the samples are known, corresponding to the sizes of the monomodal standards. However, for environmentally collected NP and MP samples such a fitting procedure might not be relevant. Whilst for sample A only 3 (as opposed to 4) populations could be resolved, for samples B and C only two populations each could be resolved (as opposed to four and three respectively) (Table 2). The Gaussian fitting is not possible when number-based PSD are transformed in mass-based PSD, since distributions get skewed. In fact, the post processing transformation of the number to mass-based PSD further reduced NTA resolution. Therefore, by analysing the mass-based PSD, it was not possible to derive a reliable % wt distribution for the different populations presented in the samples with NTA. Finally, the total particle concentration of the larger particles measured by NTA is highly overestimated, similarly to what was previously measured on the monomodal standards.

Possible alternatives to MADLS and NTA for the analysis of particles in the nanometric range are CLS, TRPS, nFCM and AF4-MALS. Interestingly, they can all resolve the 4 populations within the mix for the quadrimodal samples A and B (100–250 nm range). However, when a 60 nm particle population is added (sample C), AF4-MALS and CLS struggle to detect the 60 nm population within the mix, showing limitations to detect smaller particles in a polydisperse sample at the applied concentration. In the case of the AF4-MALS the underestimation of smaller particles is also evident in the case of the 100 nm subpopulation in samples A and B that is underestimated by 50%. The underestimation of the smaller fraction in a polymodal sample is possibly associated to the higher noise in the light scattering signal of the smaller *vs* larger particles when multiple populations are detected. In the case of CLS, post-processing data analysis is required, including a manual baseline subtraction to obtain accurate concentration results. This process is particularly hard for the 60 nm population in sample C, making it impossible to detect the CPN60 within sample C for the particle concentrations at hand (~$3.3*10^{10}$/ml). TRPS and nFCM, on the other hand, can clearly identify all the subpopulations and show agreement with the expected weight distributions, including the expected percentage of the 3 sub-populations within sample C (Table 1).

3.3. Measurement of polystyrene bimodal samples in the 200 nm – 2 μm range

As final step, we wanted to investigate how the different techniques behave in the nano to micron size-interface where many of them reach their upper limit of applicability. Three mixtures of particles of 220 nm and 2 μm were prepared for this scope, by varying the w/w % of the smaller versus the larger particles (50:50, 90:10, 99:1, see table S2). AF4-MALS was excluded from this study because their higher measurable size is well below 2 μm.

First, we visualized the monomodal particles with TEM, to verify their size and spherical shape, since EM characterization was not available in the certificate of analysis for the particles provided by Polyscience. Results are shown in Fig. 5 and reported in Table 2. We are aware that electron microscopy is not suitable for robust concentration measurements, but for educational purposes we also performed the analysis of sample D (50:50% w/w), counting more than 3800 particles. Interestingly, the % number and w/w % ratio

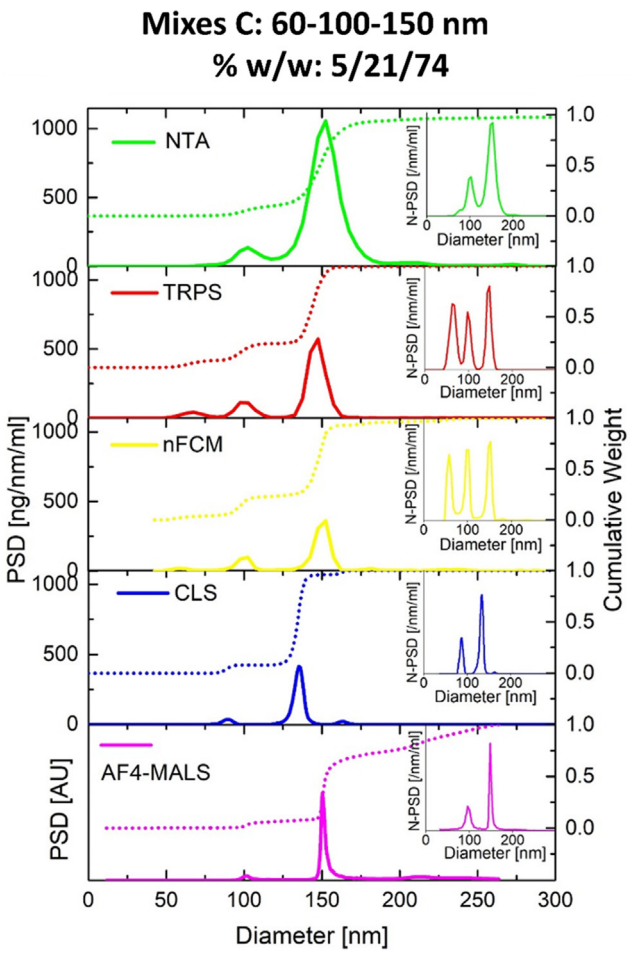

Fig. 4. NTA, TRPS, nFCM (NFC), CLS and AF4-MALS mass-based and number-based (inset) particle size distribution measurements of sample C. Differential PSD (solid lines) and cumulative PSD (dotted lines) are reported. NTA, TRPS and nFCM measurements were averaged over 3 runs and CLS over 2. For AF4-MALS PSD of a single run is reported in arbitrary units.

greatly underestimate the presence of the smaller 220 nm particles in the mixture (12/88 w/w% instead of 50/50). Smaller particles visualized in sample D (Fig. 5C), are often hidden behind the larger objects, which could partially explain their underestimation. EM, both in scanning and in transmission mode, is one of the techniques of choice for the visualization of particle morphology and for the determination of particle size distribution. If coupled with EDX it can also be used for obtaining qualitative information about the chemical composition of the particles. However, we strongly discourage to consider EM approaches (both SEM and TEM) for a quantitative estimation of the particle concentration and chemical composition.

As second step, we tested the performance of batch DLS, the most widely used analytical technique for sizing measurements worldwide, to measures samples D, E and F. Instrument providers claim that their instrument can be used for sizing measurements < 5 μm, so in theory well within our testing range with mixtures D,E and F. Is this really so? As shown in Fig. 6, Figure S3 and Figure S4, batch mode DLS does not detect the presence of the two populations in any of the mixtures tested. Very surprisingly, batch mode DLS not only does not resolve the presence of the two particle-populations, but the instrument largely underestimates the contribution of the larger, 2 μm particles in the mixtures.

In the standard DLS instrumental configuration settings (backscattering measurements at 173°, with a 633 nm laser), even when measuring sample D, the particle size distribution is still centred at around 200 nm: the diameter mode of PSD by intensity is peaked around 266 nm (Fig. 6 and Table 3). The latter results were replicated in two different laboratories as proof of their robustness (data not shown). For many of the scientists working in the nanotechnology field, including the authors, those results were unexpected at first glance, because it is usually expected that DLS tends to largely overestimate (and not underestimate!) the larger particles, due to the fact that light scattering intensity strongly increases with particle size. But here, we are beyond the true size range of applicability of batch mode DLS, and there are other important factors to consider. At particle sizes approaching the upper size range for DLS, sedimentation, thermal currents and number fluctuations start to dominate in the correlation curve *vs* the purely diffusive motion, and sizing measurements become less accurate. Severe fluctuations generate noise in the scattered intensity at the longer time points in the correlation curve (blue arrow in Figure S4, in the 10^5 μs range), which masks the fluctuations due to Brownian motion (what you want to measure). In this scenario, the system is not able to reliably perform the fitting of the data anymore, generating a completely unrealistic PSD [54,55]. Changes in the data analysis settings from general purpose to multiple narrow mode cannot improve the outcome of the calculated particle size distribution, due to the intrinsic noise of the correlogram function to be fitted. Thermal stabilization for 300 s prior to the measurements, as reported in [43] did not help to reduce fluctuation effects either.

After obtaining the first unsatisfactory results by using the most widely used instrumental setup in two different labs (Malvern Zetasizer NanoZS backscattering at 173°, 633 nm laser), we tested other configurations, e.g., varying the angle of measurement to 13° and/or using a green laser (532 nm) to investigate if DLS performance could be improved. The approach was driven by the idea of improving sensitivity toward larger particles, being guided by Mie theory, that predicts the intensity of light scattered *vs* size for particles below 50 μm (ISO 13321:2009). As demonstrated by the simulation of the scattered light *vs* size at different angles and the laser wavelength (Figure S5), when the size of the particles becomes equivalent to or greater than the wavelength of the laser (600 nm in this case), the scattering becomes a complex function with maxima and minima with respect to angle. In this context, forward scattering at 13° or the use of a smaller wavelength should help to improve sensitivity toward larger particles. As shown in Figure S3 the measurement performed with those conditions slightly improved the sensitivity toward the 2 μm population, but unfortunately the resolution power was not improved. The noise of the correlogram function was still very high and obtaining a good fitting to the data was not possible. Particle size distributions still showed very broad peaks more sensitive to larger particles (higher mode), but strongly shifted toward smaller sizes.

To conclude, in any of the tested instrumental set ups, results obtained by batch mode DLS are not reliable in the nano to micron size interface. The performances of DLS with NP & MP polydisperse samples in the nano to micron range, e.g., heterogeneous secondary MP particles produced by environmental degradation, may be even worse, due to complication induced by non-spherical morphologies. Therefore, as conclusion of this study, we would not recommend the use of batch mode DLS for analysing MP in the sub-micron range (>800 nm).

NTA, depending on the configuration setup, has a limit of applicability for larger sizes of around 600–800 nm. However, considering that its use is reported in the literature for testing secondary NP and MP samples we decided to critically evaluate its performances by analyzing a particle standard in the micrometric range before attempting the measurements of samples D-F, as reported in Figure S6. The instrument tested in this work was equipped with a

Table 1
NIST-traceable polystyrene mode diameters and measured concentration in μg/ml and in particles/ml (in brakets) of the monomodal samples CPN100, CPN150, CPN200 and CPN240, of sample A, sample B and sample C are reported. Results obtained by averaging the values extracted by the PSD of 3 runs for NTA, TRPS, nFCM and by 2 runs for CLS. For AF4-MALS values are based on 1 run. na = not available. *for all samples: particle concentration: 10^{10}/ml.

Samples/Theoretical values	Techniques	Mode diameter (nm)	% Distribution	Measured concentration μg/ml*
Name: Monomodals Size:100 or 152 or 203 or 240 nm Concentration*: 5.5/19.3/46.0/76.0 μg/ml	NTA	105/153/198/233	na	11/27/76/133 (1.1/1.39/1.85/2.06 10^{10} /ml)
	TRPS	100/151/204/244	na	6/22/53/104 (1.06/1.10/1.15/1.33 10^{10} /ml)
	CLS	93/136/184/227	na	11/15/41/69 (0.77/1.14/1.08/1.11 10^{10} /ml)
	AF4-MALS	101/151/201/241	na	NA (1.07/1.01/0.97/5.80 10^{10} /ml)
	MADLS	94/147/198/228	na	7/20/32/36 (1.43/1.20/0.85/0.62 10^{10} /ml)
	nFCM	97/147/207/242	na	4/16/35/75 (0.79/0.94/0.72/0.96 10^{10} /ml)
Name: Sample A Size: 100/152/203/240 nm w/w%: 4/13/30/53 Concentration*: 36.7 μg/ml	NTA	109/160/226*	na	64 μg/ml (1.58 10^{10} /ml)
	TRPS	107/154/207/247	3/11/28/58	36 μg/ml (0.85 10^{10} /ml)
	CLS	92/136/184/226*	8/13/26/52	28 μg/ml (0.74 10^{10} /ml)
	AF4-MALS	101/148/196/230	2/10/17/71	na (10^{10} NP/ml)
	MADLS	211	100	27 μg/ml (0.63 10^{10} /ml)
	nFCM	99/147/212/243	3/13/30/55	26 μg/ml (0.66 10^{10} /ml)
Name: Sample B Size: 100/152/203/240 nm w/w%: 2/30/43/25 Concentration*: 31.6 μg/ml	NTA	155/213	na	78 μg/ml (1.56 10^{10} /ml)
	TRPS	103/158/205/247	2/25/43/30	39 μg/ml (0.99 10^{10} /ml)
	CLS	91/136/185/225	3/28/41/28	26 μg/ml (1.02 10^{10} /ml)
	AF4-MALS	96/148/197/232	1/26/40/33	na (1.14 10^{10} /ml)
	MADLS	198	100	25 μg/ml (0.73 10^{10} /ml)
	nFCM	97/148/216/247	2/29/43/26	28 μg/ml (0.84 10^{10} /ml)
Name: Sample C Size: 60/100/152 nm w/w%: 5/21/74 Concentration: 8.7 μg/ml	NTA	102/152	10/90	28.7 μg/ml (1.88 10^{10} /ml)
	TRPS	67/102/152	7/17/76	10.9 μg/ml (1.32 10^{10} /ml)
	CLS	90/135	9/91	3.7 μg/ml (0.66 10^{10} /ml)
	AF4-MALS	101/150	9/91	na (0.77 10^{10} NP/ml)
	nFCM	60/102/152	4/21/75	6.6 μg/ml (0.74 10^{10} /ml)
	NTA	102/152	10/90	28.7 μg/ml (1.88 10^{10} /ml)

blue laser, to improve performance when analyzing smaller rather than larger particles. Thus, this setup did not perform reliably when analyzing the particles of 1 μm. The rationale behind is that the slow Brownian motion of particles of such dimensions leads to very small displacements that are difficult to distinguish from the flow of mobile phase in the measurement cell, and hence a large uncertainty in measured size. Manual settings, such as changing the sensitivity of the camera, modifying shutter, gain and the histogram of intensities captured by the camera during the recording, were tested too, but despite these attempts, it did not lead to any sensitivity improvement in the measurements. For this reason, the measurements of samples D-F were not attempted. Other instrumental configurations may be more accurate in the measurement of particles larger than 1 μm [52,53]. However, considering the great challenge for NTA in this size range, to demonstrate robustness in specific different instrumental configurations, standard particles of the same size (e.g., 1 μm) should be tested first, and measurements of unknown samples may be attempted only if the measurement accuracy, tested with the particle standards is satisfactory.

nFCM in its current configuration is optimized for the nano range and is only suitable to quantify the concentration of 200 nm particles while only size information can be provided for > 1000 nm particles. The narrow diameter of the sample stream (~1.4 μm) within the NanoAnalyzer excludes particles within the micron range, moving them into the sheath fluid and preventing damage to the Single Photon Counting Module detector. The attempts shown in the supplementary material (Table S4) to measure samples E and F, possessing low concentrations for 2 μm particles, provides an interesting first look at the potential for specialized NanoAnalyzer instruments in the micrometer range.

Additionally, conventional FCM was tested as an alternative to nFCM for the 220 nm/2 μm mixes and for concentration measurement of particles in the micron and high sub-micron range. FCM, however, could not accurately distinguish either population of particles. Various concentrations of 220 nm and 2 μm particles were

Table 2
Measured mode diameters, w/w% distributions and total concentration for mixtures D, E, F, and monomodal samples. * TRPS measures concentrations in particles/ml that were consecutively converted into mass-based concentrations, assuming a solid spherical shape and a density of 1.05 g/ml. **not able to resolve multiple peaks. ***estimated by gravimetrical sample preparation. ****measure performed on another batch of particles (Fig S6). SD = standard deviation of the mean. na = not available. DLS results acquired at 173° with a 633 nm laser are reported here. DLS = average of 5 measurements; the mode of the intensity-based PSD is reported. TRPS = average of 3 measurements for concentration and of 9 measurements for size. SLS and TEM = results of 1 measurement.

Sample	Technique	Mode diameters (SD) nm	% w/w	Concentration (SD) measured (mg/ml)	Theoretical concentration*** (mg/ml)
Mix D	**DLS**	266 (6)**	na	na	13.5/13.0
	TRPS	215(5)/1725(27)	48/52	11 (2)/12 (1)*	
	CLS	216/1729	51/49	13.4/12.7	
	SLS	132/1760	53/47	na	
	TEM	209/1979	12/88	na	
Mix E	**DLS**	243 (3)**	na	na	24.2/2.6
	TRPS	215(6)/1718(25)	90/10	20 (3) /2.3 (0.1)*	
	CLS	216/1729	90/10	22.5/2.5	
	SLS	119/1790	90/10	na	
Mix F	**DLS**	245 (2)**	na	na	26.7/0.26
	TRPS	211 (2)/1747 (25)	99/1	22 (3)/0.29 (0.03)*	
	CLS	216/1727	99/1	25.0/0.33	
	SLS**	176/1750	92/6	na	
CPN220	**DLS**	232 (3)	na	na	27
	TRPS	214 (6)	100/0	23 (5)/0*	
	CLS	216	100/0	26.4	
	SLS	117	100/0	na	
	TEM	209	100/0		
CPN*2000	**DLS**	2100 (64)	na	na	26
	TRPS	1738 (32)	0/100	0/24 (3)*	
	CLS	1721	0/100	31.4	
	SLS	1759	0/100	na	
	TEM	1979	0/100		

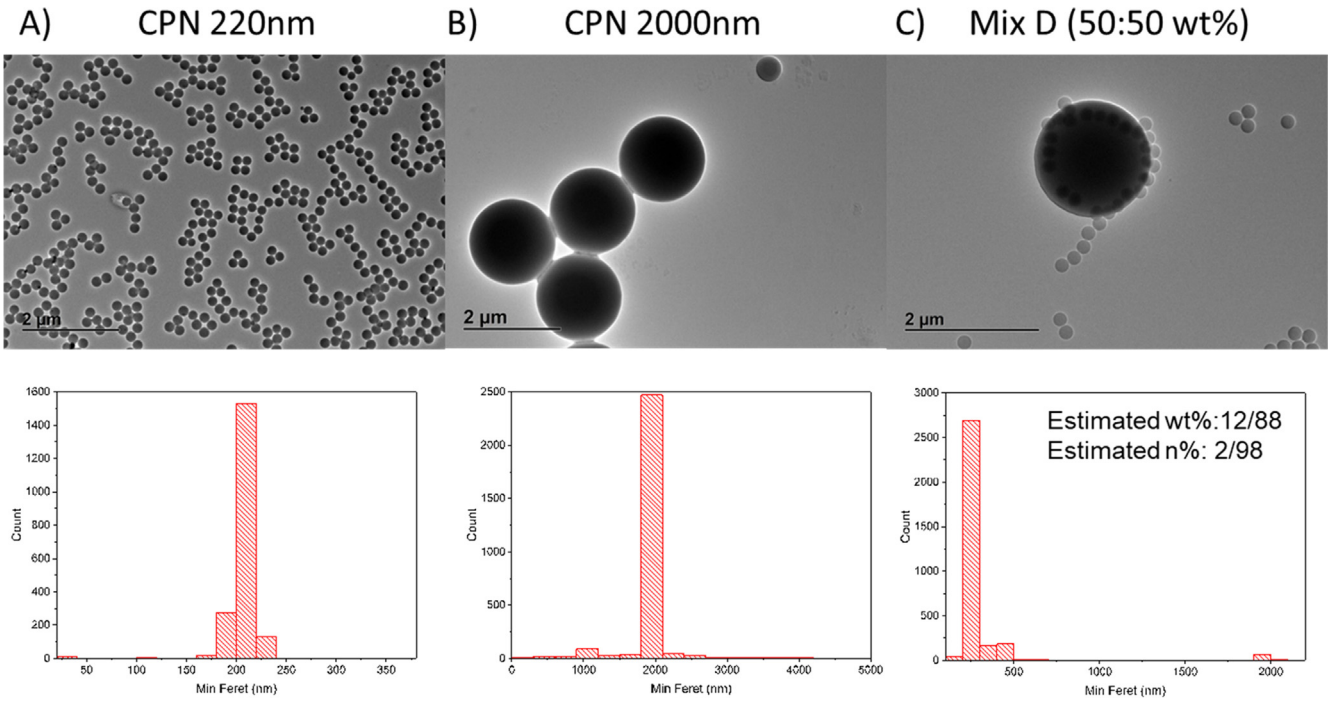

Fig. 5. TEM analysis of sample D. Images acquired for A) CPN220, B) CPN2000 and C) Mix D (50:50 wt%) are shown on the top. On the bottom respective number-based particle size distributions are reported.

tested alone and as mixtures (samples D, E, and F) and the following challenges became apparent. The 220 nm particles appeared to be at the limit of sensitivity of the instrument and could not be accurately discriminated from the background introduced by the filtered, HPLC grade water it was diluted in. The 2 µm particles also proved difficult to be resolved, as they appeared as aggregates in the dot plots with multiple populations and hence particle concentrations for the individual particles or their mixtures could not be determined accurately in any case (Figure S7).

As a final step, multiple alternatives to batch mode DLS, NTA and flow cytometry were considered for characterization. SLS may be a better light scattering based approach in the > 800 nm range. As expected, SLS was able to discriminate the two fractions at all the %wt tested but was not very precise in determining the size of the 220 nm population that is at the lower size limit of the instrument. The analysis of two different batches of 220 nm and 2 µm particles, confirmed that the mode diameter of the 220 nm particles is always slightly underestimated (Fig. 6, Figure S8

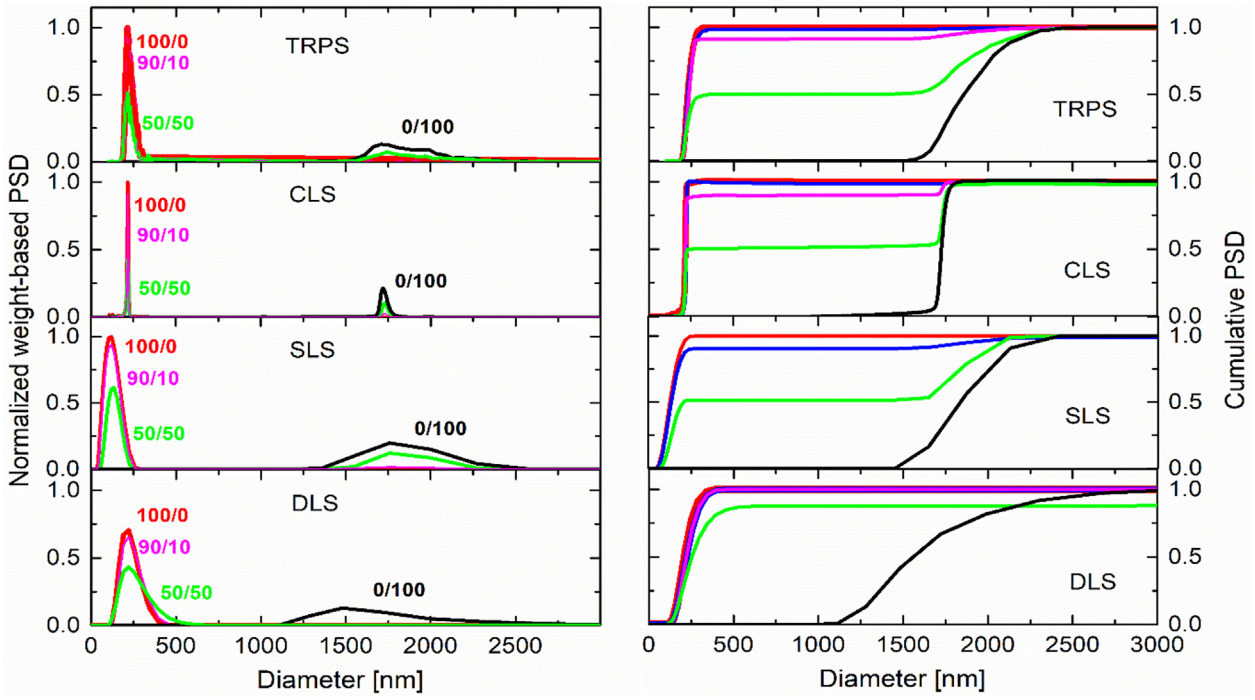

Fig. 6. Mass-based particle size distribution derived by FCM, TRPS, CLS, SLS and DLS of the bimodal samples D (50/50 w/w % of 220 nm/1.93 μm, green), E (90/10 w/w % of 220 nm/1.93 μm, pink) and F (99/1 w/w % of 220 nm/1.93 μm, blue). The measurements performed on the monomodal standards are also reported (100/0 220 nm/1.93 μm, red; 0/100 220 nm/1.93 μm, black). Normalized differential PSD (left panel) and cumulative PSD (right panel) are reported. (For interpretation of the references to colour in this figure legend, the reader is referred to the web version of this article.)

Table 3
Results obtained by the comparison of the orthogonal methods considered in this paper, according to their size range, performances in resolution for size and concentration measurements. sample needs, costs, and measurement complexity. All the categories in the table refers to the results obtained by PS standard tested in this work. Parameters such as the applicable size range, resolution, performances in concentration measurements may vary when samples of different nature (e.g., inorganic samples) are tested. Legend: na = not applicable; parameter quantification: low < moderate < medium < high.

Parameters	NTA	TRPS	DLS (MADLS)	AF4-MALS	CLS	SLS (Mastersizer)	nFCM	TEM
Applicable range*	100 nm – 800 nm	40 nm –20 μm	1 nm-800 nm	100 nm-800 nm	100 nm – 50 μm	200 nm-1000 μm	60 nm-1000 nm	>5nm**
Resolution	high	very high	Low	high	very high	high	very high	very high
Performances in total concentration measurements	medium nm (overestimation)	high	low	High for %w/w, total conc. not available	high	high for %w/w, total conc. not available	high	na
Spherical shape assumed by default?	yes	no	yes	no	no	yes	no	no
Cost per sample	low	low	very low	medium	moderate	low	low	high
Technical expertise required	moderate	moderate	low	medium	moderate	low	moderate	high
Data analysis complexity	moderate	moderate	low	medium	High (baseline subtraction)	low	moderate	medium
Calibration required	no	yes	no	no	yes	no	yes	no

and Table 2). Furthermore, concentration measurements with SLS are usually not easy to carry out, due to the unknown mass, injected in the measurement cell following a typical protocol (Mastersizer).

TRPS and CLS performed well in the measurements of all the three mixtures, being able to resolve all the populations and to precisely quantify their size and relative amount (Table 2 and Fig. 6). The measured mean diameters of various populations agree with the nominal diameters (within 10%). Moreover, the % wt ratio of the different populations was adequately measured even in the case of the more challenging 99:1 mixture (sample F), showing a high potential for mass-based concentration measurements of NP. Mass-based concentrations are typically within the expected range (within 20%) for all tested mixtures (Table 3).

4. Discussion

As shown by the results obtained in this study, each technique has its own strengths and disadvantages, in terms of ease of use, instrumental cost, range of applicability and capability to measure polydisperse samples (Table 3). In terms of applicable size ranges, SLS does work well in the micron range but is not precise with 200 nm particles, while NTA, AF4-MALS and DLS, nFCM cannot reliably measure the size and mass-based concentration of micrometric particles. Additionally, FCM has proven reliable for measuring fluorescently- stained extracellular vesicles but could not accurately determine concentrations of 220 nm or 2 μm particles via light scatter alone. TEM is the only technique that allows to visualize sample morphology but is not suitable to measure particle

concentrations. Mass-weighted PSDs can be derived from light extinction-based distributions measured by CLS, while in the case of NTA, TRPS, nFCM and MADLS it must be calculated from number-based concentrations. As a result, all these methods require information on the particle density.

The results obtained in the previous section for the measured polystyrene samples in the nano and in the sub-micron range, have underlined some method specific issues that we would like to discuss more in detail, method by method, for educational purposes before drawing the final conclusions.

DLS in batch mode, at one or at multiple angles (MADLS), is a low-resolution technique. Due to light scattering intrinsic limitation, it is not able to resolve multiple populations in a complex mixture. In the nano-range it strongly overestimates large particles due to the dependence of light scattering intensity to particle size. On the other hand, when approaching the micron range particle fluctuation starts to impact the measurements, resulting in a strong underestimation of the large particles. Despite being suggested as one of the measurement approaches of choice to measure size and particle size distribution of very small particles, we strongly discourage its use as a single analytical tool for sizing and concentration measurements of polydisperse samples or of samples containing particles > 800 nm in size.

NTA showed only a limited capability to properly resolve all the populations present in quadrimodal polystyrene mixtures < 300 nm, as shown in a previous study [50]. Multimodal Gaussian fitting could be used to determine % distributions but fittings were non-obvious and prior knowledge of the exact composition of the mixtures was required, in order to calculate % distributions reliably. Moreover, in the transformation from number-based to mass-based PSD resolution power is lost. Furthermore, NTA cannot be reliably used above 800 nm.

SLS is a better alternative to determine the size distribution and % wt of the different populations in a mix of submicron (220 nm) and micron particles (2 μm). However, sizing analysis may not be precise for particles smaller than 200 nm (diameter) where the lower sizing detection limit of this technique is reached. Moreover, since it is typically not possible to reliably quantify the mass injected in the measurement cell, no absolute concentration measurements can be performed. It should also be considered that this technique requires a relatively high amount of sample, which may not be a limitation for the characterization of raw materials intentionally added in commercial products but would be definitely be an issue for the sizing analysis of environmental MP samples.

In the nano-range, the coupling of AF4 separation to a light scattering detector (either DLS or MALS), helps to improve the intrinsic limitation of light scattering measurements in batch mode. **AF4-MALS** is therefore very well suited to measure the size of polydisperse samples in the nanometre range but presents some limitations in the measurement of mass-based particle concentrations. There are multiple reasons for this. First, the sample can be lost in the measurement process, e.g. due to the particle interactions with the membrane, that could bias the measurement of particle concentration. Secondly, there is a high uncertainty of predicting the refractive index of real-life sample particles which will crucially affect AF4-MALS concentration measurements.

TRPS resolved the size of various populations of polystyrene particles within each sample, with mode diameters in good agreement with nominal diameters, which is in line with findings reported by Anderson et al [50]. It measured mass- and number-based particle concentration very accurately, with % w/w distributions for various modes within a mix agreeing well with nominal values. If the suitable instrumental configuration is selected it can be used to measure particles from 60 nm to 20 μm and larger [48]. However is not possible to cover the complete size range with the same instrumental configuration, and the combination of multiple measurements by using different pore sizes, calibration beads and electrolyte buffers may be needed, as in the analysis of the 220 nm/ 2 μm mixtures. In order to cover particle size ranges outside the normal range of individual nanopores a panel of nanopores can be used. However, with each nanopore, a specific filtering step may have to be included before analysing samples. The filtration step will prevent particles, larger than the individual pore size, from occluding the nanopore.

CLS can also easily resolve various particle populations within samples in all the mixture tested. Mode diameters of various populations within a mix are consistently smaller (by 5–11%) than nominal diameters, possibly due to an incorrect estimation of the real density of the polystyrene nanoparticles. Provided, that PSDs are baseline-subtraction corrected (additionally to automatic baseline subtraction) and the composition (density) of the sample is well known, the measured concentrations agree with the nominal concentration and % w/w values for various modes within a mix. The fact that there is a clear need for the knowledge of the particle optical properties and density of a sample and data post-processing, PSD and concentration measurements of unknown secondary NP and MP samples using CLS will need to use independent estimations of the particle properties, including density, refractive index and absorption at the measurement wavelength (425 nm). Moreover, for an unknown sample, manual baseline subtraction cannot be performed reliably and the measurement of the quantitative contribution particular of smaller particles (100 nm and smaller) to the number- and mass-based PSD and concentration of polydisperse mixes will have a very high uncertainty. Importantly CLS is the only technique tested that directly derives mass-based PSD, without the need to transform number-based PSD into a mass-based PSD.

nFCM demonstrated a high capability to resolve monomodal and quadrimodal polystyrene particles within the nanometric range (<1000 nm), with mode diameters in good agreement (within 12%) with the nominal diameters. Concentration ratios of various sub-populations within polydisperse samples showed good accuracy and reproducibility. Flow cytometry in its nFCM variant possesses very high resolution and accuracy < 1000 nm, but due to it focused design it is not suitable for analysis of larger micrometric particles. Moreover, calibration for sizing measurements are required to share refractive indices with measured samples and may lead to uncertainty when standard particles with similar optical properties are unavailable. Concentration measurements may require two different sets of calibration, one for size and the other for concentration. Despite this, Figure S7 demonstrates that large particles were detectable for quantification and in low levels did not interfere with measurements of NPs.

FCM, while showing potential for detecting fluorescently-stained extracellular vesicles, proved unreliable for picking up accurate concentrations of particles at 200 nm or 2 μm size-range, if particles do not contain fluorescent dyes. In fact, 200 nm NP are at the very limit of sensitivity of the instrument and 2 μm MP appeared as multiple populations of aggregates and individual particles making it difficult to establish the true particle number.

TEM is obviously sub-optimal for quantitative concentration measurements. Moreover, particle aggregation on the grid during sample preparation could induce misleading results with larger particles masking smaller ones. Nevertheless, EM remains the only approach to have direct information about particle morphology. Furthermore, it can be combined with elemental analysis (e.g.,

EDX) to have qualitative information about particle chemical composition (e.g., organic *vs* inorganic materials).

5. Conclusions and outlook

Particle sizing and the measurement of mass-based particle concentration are two of the key parameters that are taken into consideration as criteria for the possible upcoming legislative restrictions of the NP and MP intentionally added in consumer products. As demonstrated in this work, the measurement of particle size distribution, and mass-based concentration is a complex task even for samples with spherical particles of known physical and chemical composition, if they are polydisperse. Bridging the gap between the nanometre and micrometre size range (800 nm-5 μm) is an even greater challenge for conventional techniques. As a general, maybe obvious conclusion, no single analytical technique evaluated fits all requirements for sizing and concentration measurements. We therefore suggest combining at least two complementary methods, to be selected on a case-by case basis depending on the sample at hand. Importantly, care should be taken not to use techniques beyond their true limit of applicability or outside their scope. In this context, we have demonstrated that light scattering sizing methods commonly used and accepted by regulatory authorities are not suitable to measure particle size and concentration accurately and reliably. Interestingly, none among DLS, FCM, NTA, AF4-MALS and nFCM in the standard configuration tested can cover the gap between the nanometre and micrometre range (800 nm- 5 μm), despite their use being proposed by multiple authors for the study of nano and microplastics [12,14,31,35,39,40,53]. Nevertheless, nFCM have shown to be very accurate if used for particles in the 60–300 nm range.

TRPS and CLS are very suitable for high-resolution particle sizing and mass-based concentration measurements over a broad size range. They reliably work both in the nanometre range when analysing complex polydisperse mixtures and in the nanometre to micrometre interface when mixtures of nanometric particles and of particles of a few micron are present. Despite their limitations, and not being mainstream approaches that you would typically find in every standard environmental analytical laboratory, they are robust and are cost-effective techniques, to be used extensively in the future for NP and MP analyses. As an alternative, simpler analytical approaches to measure particle size distribution, such as DLS or SLS, can be combined with quantitative chemical analyses, by Pyr-GC-MS, FTIR or Raman spectroscopy, to obtain sizing and mass-based concentration information from two different analytical approaches. But, sizing should be performed only with suitable and robust techniques. Care should be taken about possible misleading results obtained by mainstream light scattering techniques used outside their true range of applicability, that may differ from the one indicated by the instrumental providers.

Extra care needs to be taken when measuring samples of non-spherical morphology, where some of the techniques considered are not applicable, due to a spherical assumption assumed by default in data analysis (e.g. DLS, NTA). This is particularly critical when analysing environmental samples, presenting irregular morphologies as a consequence of the particle degradation process. Testing of polymeric samples with higher aspect ratio (e.g. rods or fibres) using various techniques, is currently ongoing and will be subject of a follow-up paper. As previously stated, sizing and mass-based concentration analysis considered here is just one of the different characterization steps, required to respond to the proposed ECHA restriction of NP and MP in consumer products. Chemical characterization should be added as complementary information, in order for example to distinguish synthetic polymer particles from inorganic particles. Chemical identification could be obtained using classical techniques (such as infrared spectroscopy, μ-Raman, NMR, pyrolysis GC-MS, and EDX) and coupled, off-line (or in-line), with size and concentration measurements.

To conclude, this work is aiming at supporting researchers in the NP and MP field, plastic producers, as well as regulatory authorities to define a robust characterization strategy for measuring particle size and mass-based concentration of NP and MP that could be applicable in the frame of the upcoming legislative restrictions. The data, here presented, provides experimental evidence to assess the relative limitations of the available techniques for sizing plastic particles in nano to micron interface. It is also expanding the landscape of available techniques for the analysis of particle size distribution and mass-based concentration beyond the commonly used light scattering techniques.

Author contribution

FC, LC, APM and RV jointly contributed to the design of the work. FC, JS, GV, JP, GH, GDC, EB, DM, JP, BP, AL, DA and OG performed the experimental work. FC drafted the manuscript. FC, RV, DM, APM and LC contributed to the manuscript revision. All the authors have approved the manuscript.

7. Disclaimer

The scientific output expressed here does not imply a policy position of the European Commission. Neither the European Commission nor any person acting on behalf of the Commission is responsible for the use that might be made of this publication.

Declaration of Competing Interest

RV is a contractor at IZON Science and JM is employed by IZON Science and their contributions to this paper were made as part of their contract/employment. AL, BP, DA are employees of nano Flow Cytometry and their contributions to this paper were made as part of their employment.

Acknowledgements

We thank Douglas Gilliland and Susanne Belz (JRC Ispra) for the useful discussion and comments. We would like to thank Dan Some from Wyatt for their excellent assistance in technical understanding and data analysis of AF4-MALS data. We thank Sylvie Motellier, CEA Grenoble, for the exchange and support during the method development of the AF4 protocol to analyze the polystyrene standards. FC acknowledge the SEP-2020 BU ref number # 102022772 for financial support. APM and JS acknowledges the partial financial support from Science Foundation Ireland for the financial support under the AMBER centre under EHS strand and Directors Fund project ref #12565. FC, APM, GH and GV acknowledges the partial financial support from the European Commission under the H2020 programme under the grant ref # 761104.

Appendix A. Supplementary data

Supplementary data to this article can be found online at https://doi.org/10.1016/j.jcis.2020.12.039.

References

[1] F.E. Heddagaard, P. Møller, Hazard assessment of small-size plastic particles: is the conceptual framework of particle toxicology useful?, Food Chem. Toxicol. 136 (2020), https://doi.org/10.1016/j.fct.2019.111106 111106.
[2] F. Barbosa, J.A. Adeyemi, M.Z. Bocato, A. Comas, A. Campiglia, A critical viewpoint on current issues, limitations, and future research needs on micro-

and nanoplastic studies: from the detection to the toxicological assessment, Environ. Res. 182 (2020), https://doi.org/10.1016/j.envres.2019.109089 109089.
[3] H. Bouwmeester, P.C.H. Hollman, R.J.B. Peters, Potential health impact of environmentally released micro- and nanoplastics in the human food production chain: experiences from nanotoxicology, Environ. Sci. Technol. 49 (2015) 8932–8947, https://doi.org/10.1021/acs.est.5b01090.
[4] Q. Zhang, E.G. Xu, J. Li, Q. Chen, L. Ma, E.Y. Zeng, H. Shi, A review of microplastics in table salt, drinking water, and air: direct human exposure, Environ. Sci. Technol. 54 (2020) 3740–3751, https://doi.org/10.1021/acs.est.9b04535.
[5] L.W.D. van Raamsdonk, M. van der Zande, A.A. Koelmans, R.L.A.P. Hoogenboom, R.J.B. Peters, M.J. Groot, A.A.C.M. Peijnenburg, Y.J.A. Weesepoel, Current insights into monitoring, Bioaccumulat. Potent. Health Effects Microplastics Present Food Chain Foods 9 (2020) 72, https://doi.org/10.3390/foods9010072.
[6] P. Alexy, E. Anklam, T. Emans, A. Furfari, F. Galgani, G. Hanke, A. Koelmans, R. Pant, H. Saveyn, B. Sokull Kluettgen, Managing the analytical challenges related to micro- and nanoplastics in the environment and food: filling the knowledge gaps, Food Addit. Contaminant: Part A 37 (2020) 1–10, https://doi.org/10.1080/19440049.2019.1673905.
[7] Y.-L. Wang, Y.-H. Lee, I.-J. Chiu, Y.-F. Lin, H.-W. Chiu, Potent impact of plastic nanomaterials and micromaterials on the food chain and human health, IJMS. 21 (2020) 1727, https://doi.org/10.3390/ijms21051727.
[8] M. Revel, A. Châtel, C. Mouneyrac, Micro(nano)plastics: a threat to human health?, Cur. Opin. Environ. Sci. Health 1 (2018) 17–23, https://doi.org/10.1016/j.coesh.2017.10.003.
[9] S. Hann, C. Sherrington, O. Jamieson, M. Hickman, P. Kershaw, A. Bapasola, G. Cole, Investigating options for reducing releases in the aquatic environment of microplastics emitted by (but not intentionally added in) products Final Report, (n.d.) 335.
[10] https://echa.europa.eu/documents/10162/05bd96e3-b969-0a7c-c6d0-441182893720 (accessed July 20, 2020).
[11] https://echa.europa.eu/registry-of-restriction-intentions/-/dislist/details/0b0236e18244cd73 (accessed October 5, 2020).
[12] https://echa.europa.eu/documents/10162/c9849410-c360-d95b-e287-ae635b0b7b3f (accessed July 20, 2020).
[13] A.N.V. Lakshmi Kavya, S. Sundarrajan, S. Ramakrishna, Identification and characterization of micro-plastics in the marine environment: a mini review, Mar. Pollut. Bull. 160 (2020), https://doi.org/10.1016/j.marpolbul.2020.111704 111704.
[14] J. Pinto da Costa, V. Reis, A. Paço, M. Costa, A.C. Duarte, T. Rocha-Santos, Micro (nano)plastics – analytical challenges towards risk evaluation, TrAC Trend. Anal. Chem. 111 (2019) 173–184, https://doi.org/10.1016/j.trac.2018.12.013.
[15] P. Li, Q. Li, Z. Hao, S. Yu, J. Liu, Analytical methods and environmental processes of nanoplastics, J. Environ. Sci. 94 (2020) 88–99, https://doi.org/10.1016/j.jes.2020.03.057.
[16] C.G. Avio, L. Pittura, G. d'Errico, S. Abel, S. Amorello, G. Marino, S. Gorbi, F. Regoli, Distribution and characterization of microplastic particles and textile microfibers in Adriatic food webs: General insights for biomonitoring strategies, Environ. Pollut. 258 (2020), https://doi.org/10.1016/j.envpol.2019.113766 113766.
[17] L. Pessoni, C. Veclin, H. El Hadri, C. Cugnet, M. Davranche, A.-C. Pierson-Wickmann, J. Gigault, B. Grassl, S. Reynaud, Soap- and metal-free polystyrene latex particles as a nanoplastic model, Environ. Sci.: Nano. 6 (2019) 2253–2258, https://doi.org/10.1039/C9EN00384C.
[18] Y. Yu, R. Ma, H. Qu, Y. Zuo, Z. Yu, G. Hu, Z. Li, H. Chen, B. Lin, B. Wang, G. Yu, Enhanced adsorption of tetrabromobisphenol a (TBBPA) on cosmetic-derived plastic microbeads and combined effects on zebrafish, Chemosphere 248 (2020), https://doi.org/10.1016/j.chemosphere.2020.126067 126067.
[19] F. Yu, Y. Li, G. Huang, C. Yang, C. Chen, T. Zhou, Y. Zhao, J. Ma, Adsorption behavior of the antibiotic levofloxacin on microplastics in the presence of different heavy metals in an aqueous solution, Chemosphere 260 (2020), https://doi.org/10.1016/j.chemosphere.2020.127650 127650.
[20] L. Sørensen, E. Rogers, D. Altin, I. Salaberria, A.M. Booth, Sorption of PAHs to microplastic and their bioavailability and toxicity to marine copepods under co-exposure conditions, Environ. Pollut. 258 (2020), https://doi.org/10.1016/j.envpol.2019.113844 113844.
[21] A.A. Koelmans, E. Besseling, A. Wegner, E.M. Foekema, Plastic as a carrier of POPs to aquatic organisms: a model analysis, Environ. Sci. Technol. 47 (2013) 7812–7820, https://doi.org/10.1021/es401169n.
[22] H. Zhang, Sorption of fluoroquinolones to nanoplastics as affected by surface functionalization and solution chemistry, Environ. Pollut. (2020), https://doi.org/10.1016/j.envpol.2020.114347 114347.
[23] K. Fikarová, D.J. Cocovi-Solberg, M. Rosende, B. Horstkotte, H. Sklenářová, M. Miró, A flow-based platform hyphenated to on-line liquid chromatography for automatic leaching tests of chemical additives from microplastics into seawater, J. Chromatogr. A 1602 (2019) 160–167, https://doi.org/10.1016/j.chroma.2019.06.041.
[24] J. Gigault, A. ter Halle, M. Baudrimont, P.-Y. Pascal, F. Gauffre, T.-L. Phi, H. El Hadri, B. Grassl, S. Reynaud, Current opinion: what is a nanoplastic?, Environ. Pollut. 235 (2018) 1030–1034, https://doi.org/10.1016/j.envpol.2018.01.024.
[25] https://phys.org/news/2019-01-dangerous-microplastic.html (accessed July 20, 2020).
[26] A. Ter Halle, L. Jeanneau, M. Martignac, E. Jardé, B. Pedrono, L. Brach, J. Gigault, Nanoplastic in the North atlantic subtropical gyre, Environ. Sci. Technol. 51 (2017) 13689–13697, https://doi.org/10.1021/acs.est.7b03667.
[27] https://www.eunomia.co.uk/reports-tools/investigating-options-for-reducing-releases-in-the-aquatic-environment-of-microplastics-emitted-by-products/ (accessed October 5, 2020).
[28] https://ec.europa.eu/environment/chemicals/reach/pdf/39168%20Intentionally%20added%20microplastics%20-%20Final%20report%2020171020.pdf (accessed July 20, 2020).
[29] S. Magalhães, L. Alves, B. Medronho, A. Romano, M. da G. Rasteiro, Microplastics in ecosystems: from current trends to bio-based removal strategies, Molecules 25 (2020) 3954, https://doi.org/10.3390/molecules25173954.
[30] https://echa.europa.eu/documents/10162/05bd96e3-b969-0a7c-c6d0-441182893720 (accessed October 5, 2020).
[31] W. Fu, J. Min, W. Jiang, Y. Li, W. Zhang, Separation, characterization and identification of microplastics and nanoplastics in the environment, Sci. Total Environ. 721 (2020), https://doi.org/10.1016/j.scitotenv.2020.137561 137561.
[32] C. Schwaferts, R. Niessner, M. Elsner, N.P. Ivleva, Methods for the analysis of submicrometer- and nanoplastic particles in the environment, TrAC Trends Anal. Chem. 112 (2019) 52–65, https://doi.org/10.1016/j.trac.2018.12.014.
[33] F. Caputo, J. Clogston, L. Calzolai, M. Rösslein, A. Prina-Mello, Measuring particle size distribution of nanoparticle enabled medicinal products, the joint view of EUNCL and NCI-NCL. A step by step approach combining orthogonal measurements with increasing complexity, J. Control. Release 299 (2019) 31–43, https://doi.org/10.1016/j.jconrel.2019.02.030.
[34] L. Calzolai, D. Gilliland, F. Rossi, Measuring nanoparticles size distribution in food and consumer products: a review, Food Addit. Contaminant.: Part A. 29 (2012) 1183–1193, https://doi.org/10.1080/19440049.2012.689777.
[35] N. Singh, E. Tiwari, N. Khandelwal, G.K. Darbha, Understanding the stability of nanoplastics in aqueous environments: effect of ionic strength, temperature, dissolved organic matter, clay, and heavy metals, Environ. Sci.: Nano. 6 (2019) 2968–2976, https://doi.org/10.1039/C9EN00557A.
[36] D. Mehn, F. Caputo, M. Rösslein, L. Calzolai, F. Saint-Antonin, T. Courant, P. Wick, D. Gilliland, Larger or more? Nanoparticle characterisation methods for recognition of dimers, RSC Adv. 7 (2017) 27747–27754, https://doi.org/10.1039/C7RA02432K.
[37] J. Gigault, H. El Hadri, S. Reynaud, E. Deniau, B. Grassl, Asymmetrical flow field flow fractionation methods to characterize submicron particles: application to carbon-based aggregates and nanoplastics, Anal. Bioanal. Chem. 409 (2017) 6761–6769, https://doi.org/10.1007/s00216-017-0629-7.
[38] G.J.A. Arkesteijn, E. Lozano-Andrés, S.F.W.M. Libregts, M.H.M. Wauben, Improved flow cytometric light scatter detection of submicron-sized particles by reduction of optical background signals, Cytometry. 97 (2020) 610–619, https://doi.org/10.1002/cyto.a.24036.
[39] M. Long, I. Paul-Pont, H. Hégaret, B. Moriceau, C. Lambert, A. Huvet, P. Soudant, Interactions between polystyrene microplastics and marine phytoplankton lead to species-specific hetero-aggregation, Environ. Pollut. 228 (2017) 454–463, https://doi.org/10.1016/j.envpol.2017.05.047.
[40] S. Summers, T. Henry, T. Gutierrez, Agglomeration of nano- and microplastic particles in seawater by autochthonous and de novo-produced sources of exopolymeric substances, Mar. Pollut. Bull. 130 (2018) 258–267, https://doi.org/10.1016/j.marpolbul.2018.03.039.
[41] C. Schwaferts, V. Sogne, R. Welz, F. Meier, T. Klein, R. Niessner, M. Elsner, N.P. Ivleva, Nanoplastic analysis by online coupling of raman microscopy and field-flow fractionation enabled by optical tweezers, Anal. Chem. 92 (2020) 5813–5820, https://doi.org/10.1021/acs.analchem.9b05336.
[42] https://www.plasticseurope.org/application/files/6315/4510/9658/Plastics_the_facts_2018_AF_web.pdf (accessed July 20, 2020).
[43] http://www.euncl.eu/about-us/assay-cascade/PDFs/Prescreening/EUNCL-PCC-001.pdf?m=1468937875&, (accessed July 20, 2020).
[44] http://www.euncl.eu/about-us/assay-cascade/PDFs/Prescreening/EUNCL-PCC-021.pdf?m=1468937875&, (accessed July 20, 2020).
[45] http://www.euncl.eu/about-us/assay-cascade/PDFs/PCC/EUNCL_PCC_023.pdf?m=1526712237&, (accessed July 20, 2020).
[46] G.S. Roberts, S. Yu, Q. Zeng, L.C.L. Chan, W. Anderson, A.H. Colby, M.W. Grinstaff, S. Reid, R. Vogel, Tunable pores for measuring concentrations of synthetic and biological nanoparticle dispersions, Biosens. Bioelectron. 31 (2012) 17–25, https://doi.org/10.1016/j.bios.2011.09.040.
[47] G.R. Willmott, R. Vogel, S.S.C. Yu, L.G. Groenewegen, G.S. Roberts, D. Kozak, W. Anderson, M. Trau, Use of tunable nanopore blockade rates to investigate colloidal dispersions, J. Phys.: Condens. Matter. 22 (2010), https://doi.org/10.1088/0953-8984/22/45/454116 454116.
[48] M. Pollard, E. Hunsicker, M. Platt, A Tunable 3D Printed Microfluidic Resistive Pulse Sensor for the Characterisation of Algae and Microplastics., ACS Sens. (2020) acssensors.0c00987. https://doi.org/10.1021/acssensors.0c00987.
[49] S.J. Sowerby, M.F. Broom, G.B. Petersen, Dynamically resizable nanometre-scale apertures for molecular sensing, Sens. Actuat. B 123 (2007) 325–330, https://doi.org/10.1016/j.snb.2006.08.031.
[50] W. Anderson, D. Kozak, V.A. Coleman, Å.K. Jämting, M. Trau, A comparative study of submicron particle sizing platforms: Accuracy, precision and resolution analysis of polydisperse particle size distributions, J. Colloid Interface Sci. 405 (2013) 322–330, https://doi.org/10.1016/j.jcis.2013.02.030.
[51] S. Gioria, F. Caputo, P. Urbán, C.M. Maguire, S. Bremer-Hoffmann, A. Prina-Mello, L. Calzolai, D. Mehn, Are existing standard methods suitable for the

evaluation of nanomedicines: some case studies, Nanomedicine. 13 (2018) 539–554, https://doi.org/10.2217/nnm-2017-0338.
[52] H. Mekaru, Effect of agitation method on the nanosized degradation of polystyrene microplastics dispersed in water, ACS Omega 5 (2020) 3218–3227, https://doi.org/10.1021/acsomega.9b03278.
[53] S. Lambert, M. Wagner, Characterisation of nanoplastics during the degradation of polystyrene, Chemosphere 145 (2016) 265–268, https://doi.org/10.1016/j.chemosphere.2015.11.078.
[54] https://www.materials-talks.com/wp-content/uploads/2018/03/FAQ-What-are-number-fluctuations.pdf (accessed October 5, 2020).
[55] https://www.malvernpanalytical.com/en/learn/knowledge-center/application-notes/AN180516LargeParticlesZetasizerUltra (accessed October 5, 2020).